

Supporting information on

Divalent cation removal by Donnan dialysis for improved reverse electrodialysis

Timon Rijnaarts^{1,2}, Nathnael T. Shenkute¹, Jeffery A. Wood³, Wiebe M. de Vos¹, Kitty Nijmeijer^{4,*}

1) Membrane Science & Technology, University of Twente, MESA+ Institute for Nanotechnology, Drienerlolaan 5, P.O. Box 217, 7500 AE Enschede, The Netherlands

2) Wetsus, European Centre of Excellence for Sustainable Water Technology, Oostergoweg 9, 8911 MA Leeuwarden, The Netherlands

3) Soft Matter, Fluidics and Interfaces, University of Twente, MESA+ Institute for Nanotechnology, Drienerlolaan 5, P.O. Box 217, 7500 AE Enschede, The Netherlands

4) Membrane Materials and Processes, Department of Chemical Engineering and Chemistry, Eindhoven University of Technology, Het Kranenveld 14, P.O. Box 513, 5600 MB Eindhoven, The Netherlands

*corresponding author: Kitty Nijmeijer (d.c.nijmeijer@tue.nl)

15 pages, 4 figures and 1 table

S1. RED model

In this work, some modifications have been made to the original model. The resistance of the river water compartment was previously estimated using molar conductivity at infinite dilution, which is only accurate below concentrations of 0.001 M. With this infinite dilution assumption, the resistance of the river water compartment is underestimated. In this study we therefore use tabulated experimental conductivity values from the CRC handbook up to 0.1 M, from which we interpolate the conductivities to calculate the resistance for the river water compartment.¹

For the salt diffusion coefficient Veerman et al. used experimental data to fit the salt diffusion coefficient (or, leakage through the membrane).² In this study the RED stack is operated in diffusion mode as well (in OCV, $I = 0A$), to check the salt diffusion coefficient. It is confirmed with experiments that the overall salt diffusion coefficient for the Fuji T1 CEM – Type I AEM pair is valid as well ($\sim 0.2 \cdot 10^{-10} \text{ m}^2/\text{s}$). The model can be operated in OCV mode if the current is set to 0, as well as at maximum power if the current is equal to $E_{\text{cell}}/2 \cdot R_{\text{stack}}$. The model parameters for the system geometry are also adapted to the physical dimensions of the membranes used.

This model is described by Veerman et al.² in detail, a brief summary is provided. Cell potential (in V) at position x in the stack can be calculated as follows:

$$E_{\text{cell}}(x) = \alpha_{\text{CEM}} \frac{RT}{F} \ln \frac{\gamma_{\text{S,Na}^+} \cdot C_{\text{S}}(x)}{\gamma_{\text{R,Na}^+} \cdot C_{\text{R}}(x)} + \alpha_{\text{AEM}} \frac{RT}{F} \ln \frac{\gamma_{\text{S,Cl}^-} \cdot C_{\text{S}}(x)}{\gamma_{\text{R,Cl}^-} \cdot C_{\text{R}}(x)} \quad (\text{S1})$$

where α_{CEM} and α_{AEM} are the permselectivities of CEM and AEM respectively, R the universal gas constant, T the temperature (K) and F the Faraday constant. γ denotes the activity coefficients for each ion (-) and C are the concentrations of NaCl at position x (mol/m^3). Subscript S and R denote seawater and river water streams respectively.

Area resistance of a cell in a RED stack at position x can be described by the following:

$$R_{\text{cell}}(x) = R_S(x) + R_R(x) + R_{\text{AEM}} + R_{\text{CEM}} \quad (\text{S2})$$

where the resistances are expressed in $\Omega \cdot \text{m}^2$ and subscripts denote seawater (S), river water (R), anion exchange membrane (AEM) and cation exchange membrane (CEM).

The area resistances of the water compartments (R_S and R_R) can be calculated as follows:

$$R(x) = f \frac{\delta}{\Delta(x) \cdot C(x)} \quad (\text{S3})$$

where f is a dimensionless obstruction factor caused by the spacer (0.726 in this study, as per Veerman), δ is the thickness of the compartment/spacer (m), Δ is the molar conductivity at position x ($\text{S m}^2/\text{mol}$) and C is the concentration of salt at position x (mol/m^3).

For maximum power densities, the area resistance of the load should be equal to the cell resistance.

Then, the local current density j (A/m^2) at position (x) will become:

$$j(x) = \frac{E_{\text{cell}}(x)}{R_{\text{cell}}(x) + R_{\text{load}}} = \frac{E_{\text{cell}}(x)}{2 \cdot R_{\text{cell}}(x)} \quad (\text{S4})$$

Power density (W/m^2) at position (x) can be calculated as follows:

$$P_d(x) = \frac{1}{2} j^2(x) \cdot R_{\text{cell}}(x) \quad (\text{S5})$$

The total power density of the full stack length P_{total} (W/m^2) can be calculated by integrating power density at position (x) over the length of the stack:

$$P_{\text{total}} = b \int_0^L P_d dx \quad (\text{S6})$$

Salt transport J ($\text{mol s}^{-1} \text{m}^{-2}$) can be calculated from the Coulombic current density and the diffusion or co-ion transport fluxes:

$$J_{\text{total}}(x) = J_{\text{coul}}(x) + J_{\text{dif}}(x) = \frac{j(x)}{F} + \frac{2D_{\text{NaCl}}}{\delta_{\text{mem}}} \cdot (C_s(x) - C_R(x)) \quad (\text{S7})$$

where D_{NaCl} is the salt diffusion coefficient (m^2/s) and δ_{mem} is the thickness of the membrane (m).

Water flow velocity v (m/s) through the stack can be calculated as follows:

$$v = \frac{\Phi}{L \cdot b} \quad (\text{S8})$$

where Φ is the flow rate (m^3/s), L the length of the cell (m) and b the width of the cell (m).

The residence time t_R (s) can be calculated as well through:

$$t_R = \frac{L \cdot b \cdot \delta}{\Phi} \quad (\text{S9})$$

To account for the salt transport through the membranes, the following mass balance equations are used to calculate the change in concentration of salt at position (x).

$$\frac{d}{dx} C(x) = \frac{b}{\Phi} J_{\text{total}}(x) \quad (\text{S10})$$

For the seawater this salt water flux is negative (concentration decrease) and for the river water it is positive (concentration increase) over the channel length x .

S2. Surface contact times and Donnan potential calculations for DD

Surface contact times

To make a comparison between the lab-scale cells and the upscaled stacks, the effective residence time is necessary. If we assume that the membrane surface is limiting the exchange of divalent cations, a surface contact time per volume can be calculated. For diffusion cells (batch):

$$\text{Cell surface contact time } \left(\frac{\text{m}^2\text{s}}{\text{m}^3} \right) = \frac{A_{\text{cell}} \cdot \tau}{V_{\text{cell}}} \quad (\text{S11})$$

where A_{cell} is the surface area of the membrane in the cell (m^2), τ is the residence time (s) and V_{cell} is the volume of the fresh water (m^3).

For stacks (continuous):

$$\text{Stack surface contact time } \left(\frac{\text{m}^2\text{s}}{\text{m}^3} \right) = \frac{A_{\text{stack}} \cdot \tau}{V_{\text{stack}}} \quad (\text{S12})$$

where A_{stack} is the total surface area of the membrane in the stack (m^2), τ is the residence time in the stack (s) and V_{cell} is the total volume of the fresh water in the stack (m^3).

For the stirred diffusion cell, the Reynolds number can be estimated as agitator³ by the following equation:

$$\text{Re}_{\text{,cell}} = \frac{D^2 N \rho}{\mu} \quad (\text{S13})$$

where Re is the dimensionless Reynolds number (-), D agitator diameter (0.03 m), N the agitator speed (500 rpm = 8.3 s⁻¹), ρ the fluid density (1000 kg/m³) and μ fluid viscosity (0.001 Ns/m²). In the cell, Re is ~7500.

For the stack, Reynolds numbers can be estimated⁴ as described by:

$$\text{Re}_{\text{stack}} = \frac{uD_h\rho}{\mu} \quad (\text{S14})$$

where Re is the dimensionless Reynolds number (-), u the average linear flow velocity (m/s), D_h is the hydraulic diameter (m), ρ the fluid density (1000 kg/m³) and μ fluid viscosity (0.001 kg/(m·s)). In the stack, Re is 2 – 10 depending on the flow velocity.

Donnan potentials and concentrations

By using Eq. 1 initial Donnan potentials can be calculated, which will elucidate the direction of cation transport in DD. DD takes place until 180 minutes ($1.8 \cdot 10^5 \text{ m}^2 \cdot \text{s} / \text{m}^3$) after which there is hardly any divalent cation present (within IC detection limits). For this time frame, Donnan potentials are calculated and show in Fig. S1. Convergence between Na^+ on the one hand and Ca^{2+} and Mg^{2+} on the other hand is observed, as the Donnan potential for Na^+ decreases because it moves downhill whereas for the divalent cations the Donnan potentials increases as they move uphill.

For the scaled-up stack there is a smaller degree of convergence observed, however, the same qualitative trend is seen. At high residence times and, therefore, low flow velocities less mixing promotion occurs. Comparing with the diffusion cells, which are well-mixed ($\text{Re} = 7500$), the stack has laminar flow and does not benefit from turbulent mixing eddies. In other words, a larger concentration gradient in the liquid is likely at larger residence times. At large residence times, it is therefore expected that the concentration gradient in the liquid and not the driving force is limiting for transport. This mass transfer limitation can be improved by enhancing mixing with,

for example, profiled membranes that promote mixing. However, the cost will be larger pressure drops in the liquid channels.

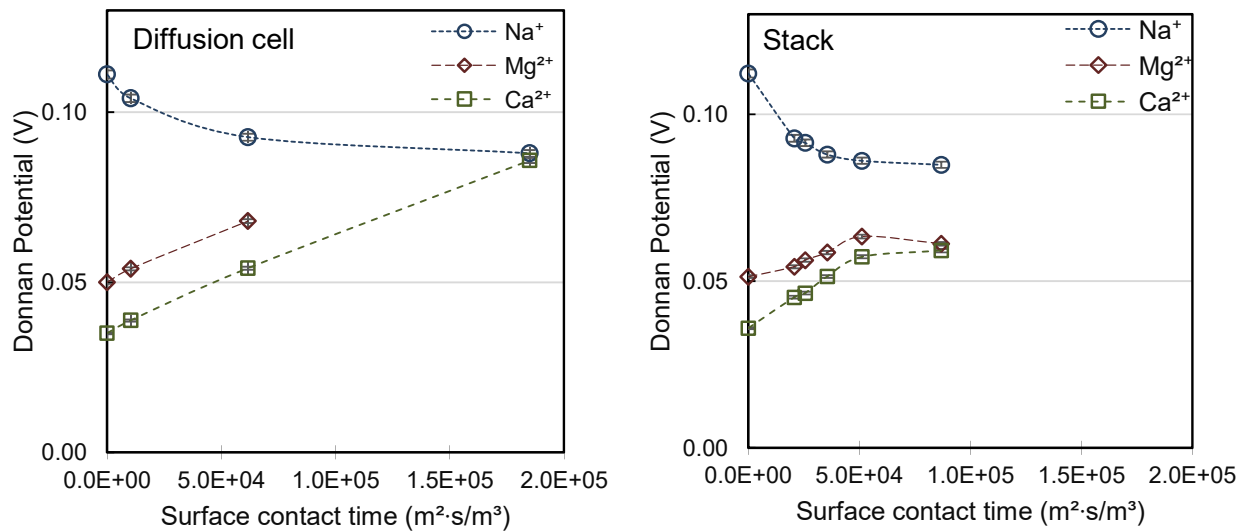


Figure S1. Donnan Potentials for each cation in the diffusion cell (left) and in the stack (right) over time for CMX. Due to Mg²⁺ concentration below the detection limit of the IC, we were unable to accurately calculate the Donnan potential after $6 \cdot 10^4$ m²·s/m³ for the diffusion cell.

Scale-up comparison for DD

In this study, experiments are performed on small-scale batch diffusion cells as well as in a continuous stack. To translate the diffusion cell experiments to similar DD divalent cation removal results in the stack, an effective surface contact time per volume of the diluate must be calculated. Residence times in the stack of several seconds should result in similar divalent cation removal as seen with diffusion cells in hours.

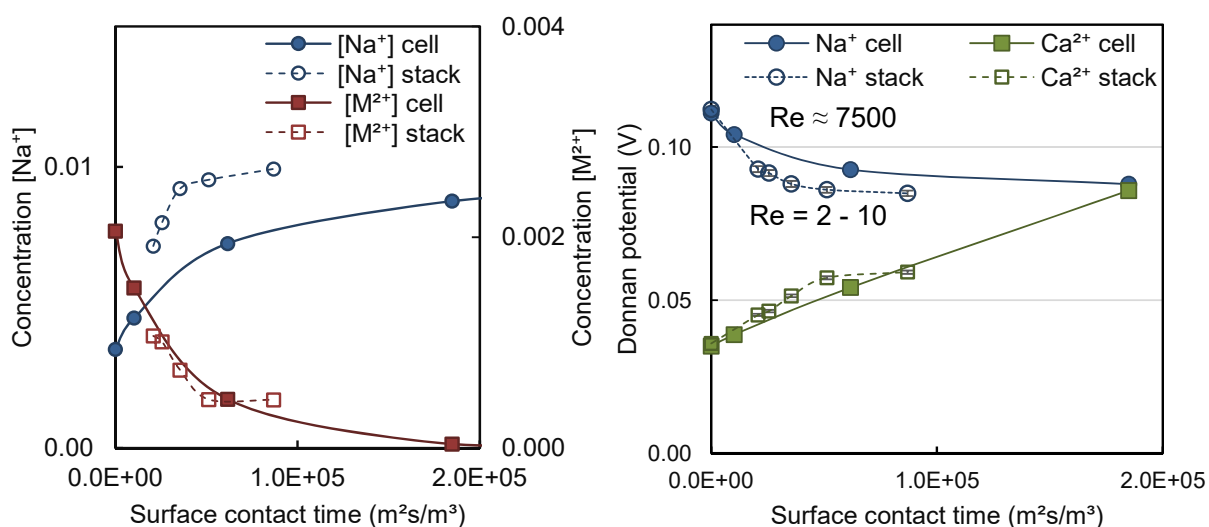


Figure S2. Concentrations vs Surface contact time (left) between lab-scale cells and scale-up stacks and Donnan potentials (right) for the cell and stack systems.

In Fig. S2, the results of this approach are shown. The divalent cation concentrations decrease at a similar rate, so removal of divalent cations is very similar. However, the sodium concentrations in the stack are significantly higher compared to the cells for the same surface contact times. This can be seen in Fig. S3 as well, where the leakage of the stack is higher (1.24 – 1.40) compared to that of the cell (1.01 – 1.14). The reason for this is the difference in mixing efficiency in the two systems. Velizarov et al. found in their study⁵ a clear dependence of DD rate on the water

compartments' Reynolds (Re) number – which is a dimensionless number for the ratio of convection to diffusion – with higher Re numbers (> 1500) leading to higher removal rates. In this study, cells have an estimated Re number of 7500, whereas the stack has Re numbers of only 2 to 10. These results indicate laminar flow profiles in the stack which cause more severe concentration polarization compared to turbulent flow profiles.⁶ Studying Donnan potentials for Na^+ and Ca^{2+} in the cell and stack can give more insight as well. In the cell, for Na^+ and Ca^{2+} the removal of Ca^{2+} is near complete at $1.8 \cdot 10^5 \text{ m}^2\text{s}/\text{m}^3$ which also is seen as the Donnan potentials are equalizing (meaning no driving force for exchange). However, in the stack it seems that concentrations as well as Donnan potentials for Na^+ and Ca^{2+} are not equal and vary hardly above $0.5 \cdot 10^5 \text{ m}^2\text{s}/\text{m}^3$. To improve the removal efficiency of the stacks to the level of well-stirred cells, mixing in the river water compartment could be improved by adding turbulence/mixing promoters in the channel (such as chevron-profiled membranes)⁷.

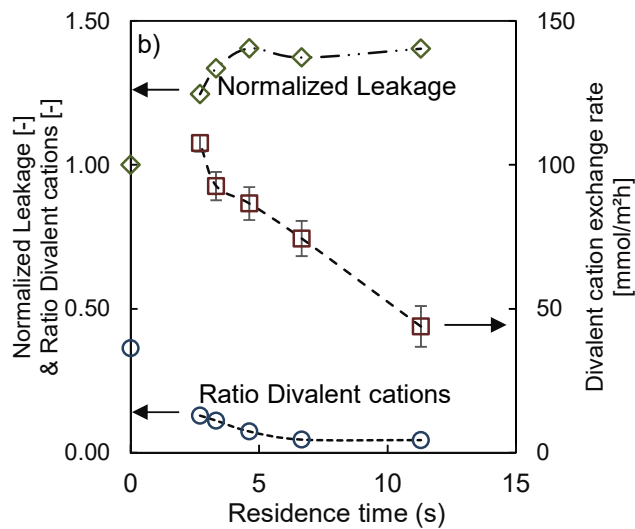
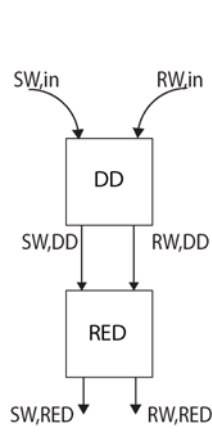


Figure S3. Leakage, divalent cation exchange rate and ratio of divalent cations in the river water as function of residence time are shown.

S3. Ionic composition of each feed stream

In Table S1, the ionic compositions of the feed, after DD pretreatment and RED outlet streams are shown. For the river water, the effect of DD is clear with a significant exchange of divalent cations for monovalent Na^+ . For seawater, the effect of DD is not significant, a small decrease of Na^+ concentration due to exchange with river water and a small increase in divalent cation concentrations is observed.

Table S1. Concentrations of all cations (in M) in the different process steps from the start (SW_{in} , RW_{in}) through DD-L (SW_{DD} , RW_{DD}) and through RED (SW_{RED} , RW_{RED}) at power harvesting conditions (20 A/m² current density). [M^{2+}] is the total divalent cation concentration.



	SW_{in}	SW_{DD}	SW_{RED}	RW_{in}	RW_{DD}	RW_{RED}
[Na^+]	0.398	0.390	0.359	0.0035	0.0099	0.0259
[K^+]	0.000	0.001	0.002	0.0007	0.0002	0.0014
[Ca^{2+}]	0.038	0.040	0.035	0.0015	0.0002	0.0011
[Mg^{2+}]	0.042	0.042	0.038	0.0005	0.0002	0.0010
[M^{2+}]	0.080	0.082	0.074	0.0020	0.0005	0.0021

Interestingly, under power harvesting conditions at a current density of 20 A/m², the divalent cation concentration is increased to 450% of the initial value (from RW_{DD} to RW_{RED}) whereas the Na^+ concentration at the outlet is 260%. There is a difference in cation transport at diffusion at OCV conditions and migration at applied current densities. This was also observed by Galama et al. during electrodialysis of seawater.⁸ The seawater after DD and RED still contains 90% of the initial cations and could be re-used for another RED stack, though with lower power densities. If

operated with “new” river water roughly 0.10 V/cell can be generated (30 - 40% less than “new” water).

S4. RED stack performance measurements for mixing of river water with some seawater

To check the effect of simply mixing some seawater with river water to increase the conductivity to the level of DD-L pretreated water, RED stack performance measurements were done. The conductivities of DD-L was 1.34 mS/cm at 25°C with only 4.3% divalent cations. Initially real river water conductivity was 1.02 mS/cm with 32% divalent cations while conductivities of the mixture (Mix) was 1.34 mS/cm at 25°C with 27% divalent cations. Conductivities (± 0.01 mS/cm) were determined by WTW Cond 3310 with 325 conductivity measurement cell.

Figure S4 shows the data for the experiments with the mixture combined with the previous results from the main paper (see Fig. 8). Especially the OCV is decreased, because of the large content of divalent cations (29%) in combination with a higher Na^+ concentration. This large content of divalent cations results in 9% loss in OCV due to uphill transport, which is similar as the untreated natural river water (with 36% divalent cations). The resistances are similar to the ones obtained using DD as pretreatment, as can be expected with similar river water conductivities. In the end, the net power densities are 0.37 W/m², which is significantly lower than all other configurations (even untreated natural water yields 0.48 W/m²).

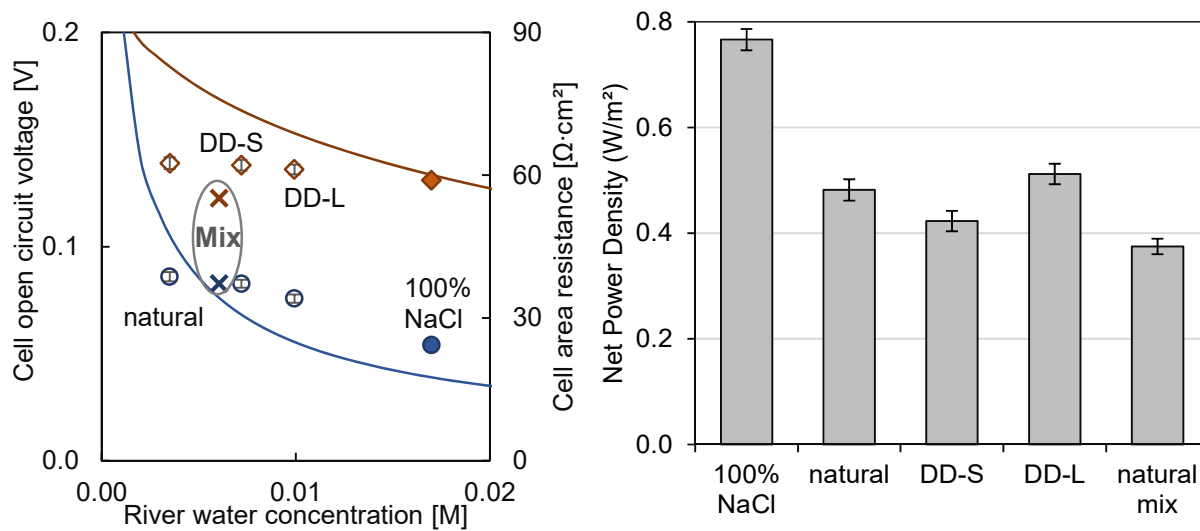


Figure S4. Data (diamonds and circles) and predictions (lines) for cell OCV and area resistance, similar as Fig. 8. The results for the mixed river water are added to both graphs. Right graph shows gross power density in grey.

References

1. *CRC Handbook of Chemistry and Physics*, . 97th Edition ed.; CRC Press/Taylor & Francis,: Boca Raton, FL., 2017.
2. Veerman, J.; Saakes, M.; Metz, S. J.; Harmsen, G. J., Reverse electro dialysis: A validated process model for design and optimization. *Chemical Engineering Journal* **2011**, *166*, (1), 256-268, DOI 10.1016/j.cej.2010.10.071.
3. Sinnott, R. K., *Chemical Engineering Design: Chemical Engineering*. Elsevier Science: 2005.
4. R. Byron Bird, W. E. S., Edwin N. Lightfoot *Transport Phenomena*. second ed.; 2007.
5. Velizarov, S.; Reis, M. A.; Crespo, J. G., Removal of trace mono-valent inorganic pollutants in an ion exchange membrane bioreactor: analysis of transport rate in a denitrification process. *Journal of Membrane Science* **2003**, *217*, (1), 269-284, DOI 10.1016/S0376-7388(03)00142-X.
6. Sonin, A. A.; Isaacson, M. S., Optimization of Flow Design in Forced Flow Electrochemical Systems, with Special Application to Electrodialysis. *Industrial & Engineering Chemistry Process Design and Development* **1974**, *13*, (3), 241-248, DOI 10.1021/i260051a009.
7. Pawlowski, S.; Rijnaarts, T.; Saakes, M.; Nijmeijer, K.; Crespo, J. G.; Velizarov, S., Improved fluid mixing and power density in reverse electro dialysis stacks with chevron-profiled membranes. *Journal of Membrane Science* **2017**, *531*, 111-121, DOI 10.1016/j.memsci.2017.03.003.
8. Galama, A. H.; Daubaras, G.; Burheim, O. S.; Rijnaarts, H. H. M.; Post, J. W., Seawater electro dialysis with preferential removal of divalent ions. *Journal of Membrane Science* **2014**, *452*, 219-228, DOI 10.1016/j.memsci.2013.10.050.